Deficiency of the bone mineralization inhibitor NPP1 protects against obesity and diabetes

Deficiency of the bone mineralization inhibitor NPP1 protects against obesity and diabetes

Carmen Huesa[# 1], Dongxing Zhu[# * 1], James D Glover[1], Mathieu Ferron [2], Gerard Karsenty [3], Elspeth M Milne [1], José Luis Millan [4], S. Faisal Ahmed [5], Colin Farquharson [1], Nicholas M. Morton [6], Vicky E MacRae [1].

[1]The Roslin Institute and Royal (Dick) School of Veterinary Studies, University of Edinburgh, Easter Bush, Roslin, Midlothian, EH25 9RG, Scotland, UK.

[2]Laboratoire de Physiologie Intégrative et Moléculaire, Institut de Recherches Cliniques de Montréal, 110 Ave. des Pins O, Montreal, Quebec, Canada H2W 1R7. Département de Médecine, Université de Montréal, C.P. 6128, succ. Centre-ville, Montréal, Québec, H3C 3J7, Canada.

[3]Department of Developmental Genetics, Columbia University, NY 10032, New York, USA.

[4]Sanford Children's Health Research Center, Sanford-Burnham Medical Research Institute, La Jolla, CA 92037, USA.

[5]Developmental Medicine, University of Glasgow, G12 8QQ, Glasgow, Scotland, UK.

[6]Centre for Cardiovascular Science, Queen's Medical Research Institute, University of Edinburgh, Edinburgh, EH16 4TJ, Scotland, UK.

Running title: The role of NPP1 in obesity and diabetes

Keywords: NPP1, mineralization, obesity and diabetes.

[#] These authors contributed equally to this work

***Address for Correspondence**

Dr Dongxing Zhu

The Roslin Institute and Royal (Dick) School of Veterinary Studies,

University of Edinburgh,

Easter Bush, Roslin, Midlothian, UK

EH25 9RG.Tel +44(0)131 6519156

Fax +44 (0)131 6519105

Email dongxing.zhu@roslin.ed.ac.uk

DMM Advance Online Articles. Posted 31 October 2014 as doi: 10.1242/dmm.017905
Access the most recent version at http://dmm.biologists.org/lookup/doi/10.1242/dmm.017905

Abstract

The emergence of bone as an endocrine regulator has prompted a re-evaluation of the role of bone mineralization factors in the development of metabolic disease. Ectonucleotide pyrophosphatase/phosphodiesterase-1 (NPP1) controls bone mineralization through the generation of pyrophosphate and is elevated in dermal fibroblast cultures and muscle of patients with insulin resistance. We investigated the metabolic phenotype associated with impaired bone metabolism in mice lacking the NPP1 gene (*Enpp1*$^{-/-}$ mice). *Enpp1*$^{-/-}$ mice exhibited mildly improved glucose homeostasis on a normal diet but showed a pronounced resistance to obesity and insulin resistance in response to chronic high fat feeding. *Enpp1*$^{-/-}$ mice had increased levels of the insulin sensitising bone-derived hormone osteocalcin but unchanged insulin signaling within osteoblasts. A fuller understanding of the pathways of NPP1 may inform the development of novel therapeutic strategies for treating insulin resistance.

Introduction

Bone remodelling is a highly conserved and regulated process that controls bone homeostasis and maintains skeletal structural integrity. This vital function is characterized by alternating phases of bone resorption by osteoclasts and bone formation by osteoblasts, and has a high energetic cost (Ducy et al., 2000). More recently it was proposed that insulin signaling mediates communication between bone remodelling and metabolic control (Fulzele et al., 2007; Lee et al., 2007; Ferron et al., 2010). Osteocalcin, a secreted protein that is specifically expressed in osteoblasts, is essential for this function of the skeleton. Hormonally active osteocalcin (in an under- or un-carboxylated form) acts to increase β-cell proliferation, insulin secretion, peripheral insulin sensitivity and energy expenditure (Ferron et al., 2008; Fulzele et al., 2010). This raises the possibility that other factors controlling bone remodelling impact upon metabolic homeostasis.

Ectonucleotide pyrophosphatase/phosphodiesterase-1 (NPP1), also known as plasma cell membrane glycoprotein 1 (PC-1), is the founding member of the NPP family, consisting of seven isozymes with a structurally related catalytic domain. The NPPs hydrolyze phosphodiester or pyrophosphate bonds in various substrates, including nucleoside triphosphates, lysophospholipids, and choline phosphate esters (Bollen et al., 2000; Stefan et al., 2000; Zimmermann et al., 2012). NPP1 is a glycoprotein that forms disulphide-bonded homodimers in the plasma membrane and mineral-depositing matrix vesicles of osteoblasts and chondrocytes (Hessle et al., 2002; Johnson et al., 2001; Terkeltaub et al., 2006; Vaingankar et al., 2004). NPP1 hydrolyzes extracellular nucleotides into inorganic pyrophosphate (PPi), a potent inhibitor of hydroxyapatite (HA) crystal formation in mineralization-competent tissues (Terkeltaub et al., 2001). Mice lacking NPP1 (*Enpp1*$^{-/-}$) have severe mineralization defects, which are associated with abnormally low PP_i levels (Anderson et al., 2005; Johnson et al., 2003; Sali et al., 1999). Phenotypic features of *Enpp1*$^{-/-}$ mice include significant alterations in the mineralization of long bones and calvaria, and pathologic perispinal soft tissue and medial arterial calcification (Mackenzie et al., 2012a; Mackenzie et al., 2012b; Sali et al., 1999).

Impaired insulin action (insulin resistance) is a significant risk factor for type 2 diabetes (DeFronzo, 1988). NPP1 negatively modulates insulin receptor signaling and has been proposed as a pathogenic factor predisposing to insulin resistance (Goldfine et al., 2008;

Prudente et al., 2009). *ENPP1* is overexpressed in skeletal muscle, adipose tissue, fibroblasts and lymphocytes of insulin-resistant individuals (Frittitta et al., 1997; Frittitta et al., 1998; Goldfine et al., 2008; Stentz et al., 2007; Teno et al., 1999). Additionally, overexpression of NPP1 in cultured cells inhibits insulin receptor autophosphorylation and downstream signaling (Grupe et al., 1995). Further studies have shown that NPP1 binds to insulin receptor and inhibits the insulin-induced conformational changes that lead to insulin receptor autophosphorylation and tyrosine kinase activation (Maddux et al., 1995; Maddux et al., 2000). Studies on the NPP1 Lys121Gln (K121Q) polymorphism (Pizzuti et al., 1999) a putative genetic determinant of human insulin resistance, led further support to NPP1 having a role in the etiology of human insulin resistance. In vitro studies have provided evidence for the increased susceptibility to insulin resistance of the Gln121 variant (Di Paola et al., 2011), with a Lys121Gln meta-analysis conducted on a European population showing a modest increase of the Gln allele in those at risk of type 2 diabetes (McAteer et al., 2008).

Despite the recognized importance of NPP1 in the control of bone mineralization, its contribution to the regulation of glucose metabolism is less clear. Given that elevated NPP1 is associated with insulin resistance (Goldfine et al., 2008; Prudente et al., 2009), we hypothesized that NPP1 gene deletion would promote improved glucose homeostasis in the context of obesity-associated diabetes. To test this we challenged *Enpp1*$^{-/-}$ mice with chronic exposure to a high fat diet.

Results

Enpp1$^{-/-}$ mice show unaltered fat mass on control diet

There was no significant difference in body weight gain from 4 weeks of age between WT and *Enpp1*$^{-/-}$ mice (Fig. 1A), yet a significant reduction in quadratus femoris muscle mass was observed from 4 weeks of age in *Enpp1*$^{-/-}$ mice (12%; $P<0.05$; Fig. 1B) with no differences in soleus muscle (Fig. 1C). The loss of muscle mass in the quadratus femoris, a key target of exercise loading, is a likely consequence of the debilitating arthritis that the *Enpp1*$^{-/-}$ mice exhibit (Filippin et al., 2013). No effect of genotype on food intake was noted. To assess onset and severity of arthritis, stride length was assessed using walking gait analysis. From 6 weeks of age, the stride length of the *Enpp1*$^{-/-}$ mice was significantly reduced ($P<0.05$), as was the progressive increase in stride length with advancing age (Fig.

1D). No differences in mRNA expression of muscle genes such as *Mstn*, *Fbxo32* or *Fndc5* were noted in these muscles (data not shown).

There were no differences in white (gonadal, subcutaneous and mesenteric) or brown fat mass (Fig. 1E) and no changes in mRNA levels of key genes for adipogenesis (*Pparg*), lipolysis (*Prkaa20*), mitochondrial metabolism (*Cpt1a*) or glucose transport (*Slc2a4*) in gonadal or brown fat mass (data not shown). However, *Cpt1a* and *Slc2a4* mRNA expression in the subcutaneous fat mass was significantly reduced in *Enpp1*$^{-/-}$ mice (50%; $P<0.05$; Fig. 1F).

Chronic deficiency of NPP1 in mice induces insulin sensitization on control diet.

Due to the recognized inhibitory activity of NPP1 on the insulin receptor (Maddux et al., 2000), we tested whether global deletion of *Enpp1* would translate into changes in whole body glucose metabolism. Adult *Enpp1*$^{-/-}$ mice showed normal glucose tolerance tests (GTT) (Fig. 2A,D) but with a lower glucose-stimulated insulin secretion (GSIS) peak across the GTT indicating insulin sensitization (Fig. 2B,D). Adult *Enpp1*$^{-/-}$ mice also showed normal insulin tolerance tests (ITT) (Fig. 2C,D) and there were no differences in insulin secreting islet size or number in the pancreas of *Enpp1*$^{-/-}$ mice (Fig. 4 E, F).

***Enpp1*$^{-/-}$ mice show obesity-resistance and improved insulin tolerance in response to chronic high fat diet challenge.**

Enpp1$^{-/-}$ mice showed resistance to weight gain caused by chronic high fat feeding compared to WT mice (Fig. 3A,B). Of note, quadratus femoris mass increased with HF diet in the *Enpp1*$^{-/-}$ mice (40% increase compared to control diet; $P<0.05$), whereas walking gait, as denoted by stride length, remained significantly reduced ($P<0.05$) (Fig. 3C).

Enpp1$^{-/-}$ mice showed reduced white adipose tissue (WAT) mass ($P<0.01$; Fig. 3D) and adipocyte cell diameter (Fig 3E). Conversely, a marked increase in brown fat mass (37%; $P<0.001$; Fig. 3F) was noted. The gonadal fat pad showed a significant increase in *PGC1α* and *Fndc5* (Fig. 3H), which are indicative of increased mitochondrial biogenesis. However there was no change in *Ucp1* mRNA levels (Fig. 3H) and hence no evidence for increased canonical thermogenesis or white fat browning as a mechanism underlying the reduced adiposity and improved metabolic profiles. In WAT, expression of white fat markers (e.g. *Cpt1*; *Prkaa2*) remained unaltered with HF diet (Fig. 3G-H). Moreover, micro-vesicular fat in

the liver, as detected by oil red O staining, was notably reduced in *Enpp1*$^{-/-}$ mice in comparison to WT littermates (Fig. 3I). No gross effect of high fat diet challenge was seen on kidney, brain, cardiovascular or muscle tissue architecture in either genotype.

Glucose tolerance was comparable between genotypes (Fig. 4A,D). However, the insulin level (GSIS) across the GTT was lower in *Enpp1*$^{-/-}$ mice, indicating potential insulin sensitization (Fig. 4B,D). Improved *Enpp1*$^{-/-}$ insulin sensitivity was confirmed by an insulin tolerance test (Fig. 4C,D). Compared to wild type control mice, no significant differences in insulin secreting islet size or number in the pancreas of *Enpp1*$^{-/-}$ mice were observed (Fig. 4 E, F).

Do osteoblasts regulate insulin sensitivity in the *Enpp1*$^{-/-}$ mice?

Given that NPP1 is a negative regulator of insulin signaling, we investigated whether osteoblast insulin signaling might link NPP1 deficiency and improved whole glucose homeostasis. Initially, we considered the distribution (Fig. 5A) and mRNA expression (Fig 5B) of the insulin receptor in confluent monolayers of primary calvarial osteoblasts, with no effect of genotype observed. Furthermore there was no effect of NPP1 deletion on insulin-stimulated Akt, Erk1/2 or GSK3β phosphorylation between *Enpp1*$^{-/-}$ and WT primary calvarial osteoblasts cultured in vitro (Fig. 5C). However, at 12 weeks of age *Enpp1*$^{-/-}$ mice exhibited increased concentrations of the osteoblast-derived insulin sensitizing hormone undercarboxylated (GLU13) (119%, $P<0.05$; Fig. 5D) and uncarboxylated (GLU) (156%, $P<0.05$; Fig. 5E) osteocalcin, while carboxylated (GLA13) and total osteocalcin levels were comparable to WT (Fig. 5F,G). Additionally, the degree of osteoblast and osteoclast activity was assessed by ELISA analysis of serum from *Enpp1*$^{-/-}$ and WT mice. No changes in the bone formation marker P1NP were noted (Fig. 5H), whereas a significant increase in the bone resorption marker CTx was observed in *Enpp1*$^{-/-}$ mice compared to WT controls ($P<0.05$; Fig. 5I). Together these data suggest that the increase in undercarboxylated osteocalcin detected in *Enpp1*$^{-/-}$ mice as a result of increased bone resorption may induce the altered insulin sensitivity phenotype observed.

Chronic high fat diet challenge induces brittle bone formation in WT mice and exacerbates the bone phenotype of *Enpp1*$^{-/-}$ mice.

Given the detrimental effects of obesity on bone (Leslie et al., 2012), we next considered the effects of chronic high fat challenge on the bone physiology of the *Enpp1*$^{-/-}$ mouse.

Following a chronic high fat diet challenge, trabecular bone in WT mice showed a significantly altered microarchitecture resulting in thinner and more disorganized trabeculi, compared with mice reared on a control diet (Table 1). Cortical bone in WT mice fed a high fat diet showed a significantly increased bone mineral density compared with mice reared on a control diet (BMD; $P<0.01$). However, cortical thickness was unchanged by the high fat diet resulting in a more brittle bone as determined by the significantly decreased work to fracture ($P<0.05$) and post-failure work ($P<0.05$) observed in the three point bending analysis (Table 1).

Enpp1$^{-/-}$ mice displayed a significant deterioration of the already compromised trabecular architecture following a chronic high fat diet challenge, as exemplified by the significant loss of connectivity indicated by the trabecular pattern factor, the loss of trabecular bone as measured by percentage of bone volume (BV/TV) and the reduced trabecular organization when compared to control diet mice (Table 1 and Fig. 6A-D). The tibiae of *Enpp1*$^{-/-}$ mice displayed a significantly reduced cortical thickness (10%; $P<0.01$). This also translated into a weaker, more brittle bone as measured by three point bending parameters whereby the work to fracture and post-failure was significantly reduced by 34% and 50% respectively ($P<0.05$; Table 1). A high fat diet challenge also induced a significant decrease in bone modelling in *Enpp1*$^{-/-}$ mice, as indicated by the significant reduction in P1NP as a marker of bone formation (38%; $P<0.001$; Fig. 6E) and CTX as a marker of bone resorption (20%; $P<0.001$; Fig. 6F). These unique data highlight that a chronic high fat challenge has critical effects on the severity of the *Enpp1*$^{-/-}$ bone phenotype.

Discussion

The role of NPP1 in controlling the pace of bone mineralization has been firmly established through the study of in vivo mouse models. This enzyme is crucial for the regulation of bone mineralization through the generation of PPi from nucleotide precursors. *Enpp1*$^{-/-}$ mice display a distinct phenotype, including altered long bone and calvarial mineralization, and pathologic soft tissue calcification (Mackenzie et al., 2012a; Mackenzie et al., 2012b; Sali et al., 1999). The necessity of NPP1 for physiological skeletal mineralization combined with the considerable evidence linking NPP1 expression with insulin resistance (Bacci et al., 2007; Baratta etal., 2008; Chandalia et al., 2012; González-Sánchez et al., 2008; Harmey et al.,

2004), led us to investigate whether NPP1 has a functional role in bone as a novel regulator of energy metabolism.

In the present study we have examined the full impact of chronic suppression of NPP1 and provide new evidence demonstrating that ablation of the bone mineralization inhibitor NPP1 protects against insulin resistance, obesity and diabetes. *Enpp1*$^{-/-}$ mice exhibited insulin sensitization, and in response to a chronic high fat diet challenge displayed improved insulin tolerance and pronounced obesity-resistance. These novel data extend recent in vitro studies where the suppression of NPP1 expression in liver, skeletal muscle and pancreatic beta-cells improved insulin sensitivity (Di Paola et al., 2011). The observation of enhanced insulin sensitivity following adenoviral knockdown of liver NPP1 expression in a mouse model of diabetes (db/db) (*Lepr*$^{-/-}$) further supports our findings (Zhou et al., 2009). In comparison with db/db mice treated with a control virus, db/db mice treated with the *Enpp1*shRNA adenovirus had 80% lower hepatic *Enpp1* mRNA levels, 25% lower fasting plasma glucose and significantly improved glucose tolerance. This critical paper (Zhou et al., 2009) highlights the bone independent effects of NPP1, and together with our findings, supports the proposition that NPP1 inhibition is a potential therapeutic approach for the treatment of type 2 diabetes.

The present study provides the first demonstration of an association between osteocalcin carboxylation status and NPP1. *Enpp1*$^{-/-}$ mice presented with increased levels of undercarboxylated osteocalcin and the bone resorption marker CTX. These data support recent findings indicating that insulin signaling in osteoblasts favors bone resorption by osteoclasts, with decarboxylation of osteocalcin occurring in resorption lacunae, resulting in increased circulating undercarboxylated osteocalcin and a positive feedback loop on insulin secretion (Ferron et al., 2010; Lacombe et al., 2013). However, our studies undertaken in calvarial osteoblast cultures did not reveal a role for NPP1 as a modulator of insulin signaling in osteoblasts in vitro, suggesting that this model may not fully reflect osteoblast activity in vivo. Further studies involving the specific knockout of the insulin receptor in *Enpp1*$^{-/-}$ osteoblasts are therefore required to categorically confirm these data. Given the recent important observation that osteoclasts regulate energy metabolism (Lacombe et al., 2013), it is also vital to determine whether *Enpp1*$^{-/-}$ osteoclasts show any functional defects.

The distinct phenotype of the *Enpp1*$^{-/-}$ mouse may also directly influence the metabolic parameters observed in the present study. *Enpp1*$^{-/-}$ mice showed reduced body weight, decreased stride length and significant muscle reduction. These data are highly compatible with the observed osteoarthritic phenotype (Mackenzie et al., 2012a; Sali et al., 1999), which may modulate the insulin sensitization induced by NPP1 loss. Indeed, metabolic osteoarthritis (OA) has now been characterized as a subtype of OA, and has been highlighted as a new facet of the definition of Metabolic Syndrome, supported by its strong associations and shared mechanisms with other Metabolic Syndrome components (Zhuo et al., 2012). Further research, however, is needed to define the reciprocal influence of OA on the currently accepted components of Metabolic Syndrome, and the putative role of NPP1.

The insulin sensitized phenotype observed in the *Enpp1*$^{-/-}$ mice may be a direct consequence of NPP1 ablation in insulin sensitive tissues such as liver, adipose and skeletal muscle. Overexpression of NPP1 in liver and muscle induces insulin resistance and hyperglycemia (Maddux et al., 2006). Moreover, overexpression of NPP1 in adipocytes leads to adipose insulin resistance, reduction in fat cell lipid storage and systemic insulin resistance and glucose intolerance akin to the effects of lipodystrophy (Pan et al., 2011). Our data support a beneficial effect of NPP1 deficiency being manifested potentially through improved insulin sensitivity in liver, muscle and adipose. However, one key difference in the *Enpp1*$^{-/-}$ mice is that insulin sensitization is associated with pronounced reduction in adipose tissue lipid storage without ectopic lipid accumulation in other organs. This suggests an overarching beneficial effect of *Enpp1* deficiency on energy expenditure that likely involves other tissues. This may include increased muscle mitochondrial biogenesis through PGC1-α, a key regulator of energy metabolism (Ferron et al., 2012) or effects of increased bone turnover. Tissue specific ablation of NPP1 is therefore required in future work to pinpoint the individual tissue(s) driving the metabolic phenotype of the *Enpp1*$^{-/-}$ mouse. Furthermore, the association of the NPP1 K121Q polymorphism with insulin resistance in several human populations (Baratta et al., 2008; Stolerman et al., 2008) highlights the need for further studies specifically investigating the impact of this variant of NPP1 on metabolism. One of the premises of targeting NPP1 as treatment to type 2 diabetes-induced insulin resistance is that the inhibition of insulin receptor and NPP1 interactions happens independently of its pyrophophosphatase/phosphodiesterase activity, although the exact mechanism is still unknown (Chin et al., 2009).

Obesity is linked to normal or higher BMD accompanied by a paradoxical increase in fracture risk (Leslie et al., 2012). Our studies mimic this clinical setting of an obesity-induced bone phenotype in the WT mouse, where the bone is more brittle despite a higher BMD. Furthermore, our data show that a HFD challenge induces a decrease in bone modelling which results in an enhanced deterioration of bone architecture and mechanical properties, which are even more pronounced in the *Enpp1*$^{-/-}$ mice. This latter observation may reflect the abnormally low levels extracellular PPi observed in these mice, which would result in insufficient PPi substrate for TNAP to generate Pi for normal mineral formation, as previously discussed (Anderson et al., 2005). Furthermore, an accumulation of nucleotide triphosphates due to lack of hydrolysis by NPP1 (Prosdocimo et al., 2009) may have a downstream effect on bone remodelling through purinergic signaling (Orriss et al., 2011). No differences in cortical porosity were seen between either genotype or diet, however it was not possible to distinguish between vascularity, osteocyte lacunae and areas of non-mineralized matrix at the resolution examined. Further investigations specifically examining these individual components using nanoCT would therefore be of great interest.

In conclusion, our data adds to the body of evidence (Goldfine et al., 2008; Prudente et al., 2009) supporting NPP1 deficiency as protective against insulin resistance. We demonstrate for the first time that ablation of NPP1 alters osteocalcin carboxylation status, whilst protecting against obesity and diabetes (Fig. 7). A fuller understanding of the pathways of NPP1 may inform the development of novel therapeutic strategies for treating insulin resistance.

Materials and Methods

Animal model

The generation and characterization of germline *Enpp1*$^{-/-}$ mice have been reported previously (Mackenzie et al., 2012a; Sali et al., 1999). Heterozygote breeders were used to generate distinct litters. Offspring carrying the mutant *Enpp1* gene were identified by PCR and performed by performed by Genetyper (Genetyper, New York,USA). Male mice were fed a high fat diet (HFD, 58% fat, DBM Scotland, Broxburn, UK) or control diet (6.2% fat, Harlan Laboratories, Indianapolis, IN, USA) from 4 weeks of age. Ad libitum food consumption was monitored for 6 days. Progression of arthritis was assessed with a non-automated “cat-walk” walking gait test, which measured the distance between the central pads of two alternating

hind footprints (Parvathy et al., 2013). All animal experiments were approved by The Roslin Institute's Animal Users Committee and the animals were maintained in accordance with UK Home Office guidelines for the care and use of laboratory animals.

Glucose and Insulin tolerance tests

Juvenile and adult (6 and 16 week old respectively) male mice were fasted for 4 hours and administered 2 mg of D-glucose (Sigma, Poole, UK) per g of body weight by gavage. 16 week old male mice were fasted for 4 hours and administered 0.5 (control diet) or 0.75 (HFD) mU of insulin (Actrapid, NovoNordisk, Bagsvaerd, Denmark) per g of body weight, while 6 week old male mice were administered 0.375 mU of insulin per g of body weight intraperitoneally (ip). At 0, 15, 30, 60 and 120 minutes intervals after administration blood glucose was measured with an Accu-Chek® Aviva glucose meter (Roche Diagnostics Ltd., Lewes, UK) and insulin was measured by ELISA (ChrystalChem, Chicago, IL, USA). Animals were subsequently sacrificed at 7 and 18 weeks of age respectively to allow for recovery from the tests. Tissues including pancreas, liver, quadratus femoris, soleus muscle and tibiae as well as brown, subcutaneous, mesenteric and gonadal fat pads were collected for histological assessment and gene expression analysis.

Primary osteoblast cell culture

Primary osteoblasts (pOBs) were isolated the calvariae of 3-5 day-old wild-type (WT) and *Enpp1*$^{-/-}$ mice as previously described (Huesa et al., 2010; Staines et al., 2013). Cells were seeded at a density of $2.5x10^4/cm^2$ in multi-well plates, in growth medium consisting of α-MEM (Invitrogen, Paisley, UK) supplemented with 10% FBS (Invitrogen) and 1% gentamicin (Invitrogen). Cells were maintained in 95% air/5% CO_2 at 37°C.

Cell signaling immunoblotting

Following confluency, pOBs were cultured for 24 hours in serum free medium containing 0.1% bovine serum albumin (BSA). Cells were then either lyzed immediately or stimulated with insulin (10 nM; Sigma) or IGF-I (10 nM; Sigma) for 10 minutes before lysis. Cells were lysed in RIPA buffer (Invitrogen) containing "phosphatase inhibitor cocktail 2" (Sigma) and "complete" protease inhibitor cocktail (Roche) according to manufacturers' instructions. Immunoblotting with specific antibodies against phospho-Akt^{ser473}, total Akt, phospho-GSK3β^{ser9}, total GSK3β phospho-Erk 1/2$^{thr202/tyr204}$ and total Erk1/2 (Cell Signaling, Boston, MA, USA). Immunoblotting was conducted as previously described (Zhu et al., 2011; Zhu et

al., 2013) and visualized using the enhanced chemi-luminescence (ECL) Western Blotting Detection System (GE Healthcare, Chalfont St Giles, UK).

RNA extraction and qPCR

Bone and fat tissues were extracted using Qiazol (Qiagen, Valencia, CA, USA) following standard protocol procedures. All other tissues and cell cultures were extracted with the RNeasy Qiagen kit following manufacturer's instructions (Qiagen). RNA was quantified and reverse transcribed as previously described (Mackenzie et al., 2011; Macrae et al., 2009). All genes were analyzed with the SYBR green detection method (Roche) using the Stratagene Mx3000P real-time QPCR system (Agilent Technologies, Santa Clara, CA, USA). All gene expression data were normalized against *Atp5B* (Primer Design, Southampton, UK; sequence not disclosed) in osteoblasts, *LRP10* in adipose tissue and *Gapdh* (Primer Design; sequence not disclosed) in all other tissues. The control values were expressed as 1 to indicate a precise fold change value for each gene of interest. All primer sequences were obtained from the Harvard primer bank database (http://pga.mgh.harvard.edu/primerbank/index.html, see supplementary material Table S1).

Tissue histology and cell immunofluorescence

Dissected tissues were fixed in 4% paraformaldehyde (PFA) or 10% phosphate buffered formalin (pH 7.4) and embedded in paraffin wax. 5 µm sections were stained with haematoxylin and eosin (H&E). Fresh tissues for lipid staining were collected immediately after euthanasia, snap frozen in precooled isopentane and stored at -80°C for less than 1 month. Cryostat sections (10µm) were stained routinely for lipid with Oil Red O. Cells were plated onto glass cover slips, fixed in 4% PFA and permeabilized with 0.1% Triton in PBS prior to insulin receptor immunofluorescent staining following standard protocols (Huesa et al., 2010).

Measurement of islet number and size

Serial sections were cut through each pancreas at 100µm intervals, stained with H&E and scanned with a Nikon CoolScan V (Nikon, Surrey, UK). The total area of a stained pancreas section was measured along with the number and size of the islets in that section using ImageJ software (Wayne Rasband, National Institute of Health, USA). At least five randomly selected serial sections were examined per pancreas and three mice were analyzed for each diet/genotype group.

Micro-computed tomography (µCt) and mechanical testing of tibiae

Tibiae were dissected and immediately frozen in PBS at -20°C pending analysis. High resolution scans with an isotropic voxel size of 5 µm were acquired with a micro-computed tomography system (µCT, 60 kV, 0.5 mm aluminium filter, 0.6 ° rotation, Skyscan 1172, Brukker microCT, Kontich, Belgium). Scans were reconstructed using NRecon software (Brukker microCT). For each bone, a 1000 µm section of the metaphysis was taken for analysis of trabecular bone, using the base of the growth plate as a standard reference point. A further 1500 µm below the base of the metaphysis section a 400 µm section of the mid-diaphysis was scanned for analysis of cortical structure. Data was analyzed with CtAn software (Brukker microCT). Cortical porosity was measured in the 2D slice by slice analysis. Binarized objects were identified containing fully enclosed spaces, and porosity was calculated as the area of those spaces as a percent of the total area of binarized objects. It should be noted that for this study, total porosity is a measurement of all of the space within the cortical bone not filled by mineral e.g. a blood vessel canal, a large osteocyte lacuna or a crack. Mechanical testing of the cortical bone was assessed by 3 point bending analysis using a Zwick materials testing machine (Zwick A.G., Ulm, Germany) with a 50 N loading cell, where the span was set at 5.5 mm and the cross-head speed was set at 1mm/min. Data was analyzed as previously described (Huesa et al., 2011).

Serum measurements

Immediately following euthanasia, blood was obtained from non-fasted 6 and 12 week old male mice and serum samples prepared. Total, carboxylated (GLA), undercarboxylated (GLU13-OCN) and uncarboxylated (GLU) osteocalcin was measured as previously described (Ferron et al., 2010), as well as markers of bone formation (P1NP; IDS, Boldon, UK) and resorption (Ctx; IDS).

Statistics

Standard comparisons between WT and *Enpp1*$^{-/-}$ mice were analyzed by unpaired Student *t*-test. Comparisons between genotype and diet were analyzed with two-way ANOVA. Time course experiments were analyzed with a repeated measures two-way ANOVA. Analysis was carried out using SigmaStat 12.0 (Systat Software Inc, London, UK).

Acknowledgements

This work was supported by an Institute Strategic Programme Grant and Institute Career Path Fellowship funding from the Biotechnology and Biological Sciences Research Council (BBSRC) and a project grant from Medical Research Scotland.

Competing interest's statement

The authors declare no conflicts of interest

Author contributions

V.E.M supervised the project, C.H, N.M.M and V.E.M conceived and designed experiments and wrote the manuscript; M.F, D.Z, E.M.M and J.G performed experiments and analyzed the data; D.Z, M.F, G.K, E.M.M, J.L.M, S.F.A, and C.F helped to prepare the manuscript. All authors read, discussed and edited the manuscript.

References

1. **Anderson, H. C., Harmey, D., Camacho, N. P., Garimella, R., Sipe, J. B., Tague, S., Bi, X., Johnson, K., Terkeltaub, R., Millán, J. L.** (2005). Sustained osteomalacia of long bones despite major improvement in other hypophosphatasia-related mineral deficits in tissue nonspecific alkaline phosphatase/nucleotide pyrophosphatase phosphodiesterase 1 double-deficient mice. *Am J Pathol.* 166, 1711-1720.
2. **Bollen, M., Gijsbers, R., Ceulemans, H., Stalmans, W. and Stefan, C. (2000).** Nucleotide pyrophosphatases/phosphodiesterases on the move. *Crit Rev Biochem Mol Biol.* 35, 393-432.
3. **Baratta, R., Rossetti, P., Prudente, S., Barbetti, F., Sudano, D., Nigro, A., Farina, M. G., Fabio, P., Trischitta, V. and Frittitta, L.** (2008). Role of the ENPP1 K121Q polymorphism in glucose homeostasis. *Diabetes.* 57, 3360-3364.
4. **Bacci, S., De Cosmo, S., Prudente, S. and Trischitta, V.** (2007). ENPP1 gene, insulin resistance and related clinical outcomes. *Curr Opin Clin Nutr Metab Care.* 10, 403-409.
5. **Chandalia, M., Davila, H., Pan, W., Szuszkiewicz, M., Tuvdendorj, D., Livingston, E. H. and Abate, N.** (2012). Adipose tissue dysfunction in humans: a potential role for the transmembrane protein ENPP1. *J Clin Endocrinol Metab.* 97, 4663-4672.
6. **Chin, C. N., Dallas-Yang, Q., Liu, F., Ho, T., Ellsworth, K., Fischer, P., Natasha, T., Ireland, C,, Lu, P., Li, C., et al.** (2009). Evidence that inhibition of insulin receptor signaling activity by PC-1/ENPP1 is dependent on its enzyme activity. *Eur J Pharmacol.* 606, 17-24.
7. **DeFronzo, R. A.** (1988). Obesity is associated with impaired insulin-mediated potassium uptake. *Metabolism.* 37, 105-108.
8. **Ducy, P., Schinke, T. and Karsenty, G.** (2000). The osteoblast: a sophisticated fibroblast under central surveillance. *Science.* 289, 1501-1504.
9. **Di Paola, R., Caporarello, N., Marucci, A., Dimatteo, C., Iadicicco, C., Del Guerra, S., Prudente, S., Sudano, D., Miele, C., Parrino, C., et al.** (2011). ENPP1 affects insulin action and secretion: evidences from in vitro studies. *PLoS One.* 6, e19462.
10. **Ferron, M., and Lacombe, J**. (2014). Regulation of energy metabolism by the skeleton: Osteocalcin and beyond. *Arch Biochem Biophys.*
11. **Ferron, M., Hinoi, E., Karsenty, G. and Ducy, P.** (2008). Osteocalcin differentially regulates beta cell and adipocyte gene expression and affects the development of metabolic diseases in wild-type mice. *Proc Natl Acad Sci U S A.* 105, 5266-5270.

12. **Ferron, M., Wei, J., Yoshizawa, T., Ducy, P. and Karsenty, G.** (2010). An ELISA-based method to quantify osteocalcin carboxylation in mice. *Biochem Biophys Res Commun.* 397, 691-696.
13. **Ferron, M., McKee, M. D., Levine, R. L., Ducy, P. and Karsenty, G.** (2012). Intermittent Injections of Osteocalcin Improve Glucose Metabolism and Prevent Type 2 Diabetes in Mice. *Bone.* 50, 568-575.
14. **Fulzele, K., DiGirolamo, D. J., Liu, Z., Xu, J., Messina, J. L. and Clemens, T. L.** (2007). Disruption of the insulin-like growth factor type 1 receptor in osteoblasts enhances insulin signaling and action. *J Biol Chem.* 282, 25649-25658.
15. **Filippin, L. I., Teixeira, V. N., Viacava, P. R., Lora, P. S., Xavier, L. L. and Xavier, R. M. (2013).** Temporal development of muscle atrophy in murine model of arthritis is related to disease severity. *J Cachexia Sarcopenia Muscle.* 4, 231-8.
16. **Frittitta, L., Spampinato, D., Solini, A., Nosadini, R., Goldfine, I. D., Vigneri, R. and Trischitta, V.** (1998). Elevated PC-1 content in cultured skin fibroblasts correlates with decreased in vivo and in vitro insulin action in nondiabetic subjects: evidence that PC-1 may be an intrinsic factor in impaired insulin receptor signaling. *Diabetes.* 47, 1095-1100.
17. **Frittitta, L., Youngren, J. F., Sbraccia, P., D'Adamo, M., Buongiorno, A., Vigneri, R., Goldfine, I. D. and Trischitta V.** (1997). Increased adipose tissue PC-1 protein content, but not tumour necrosis factor-alpha gene expression, is associated with a reduction of both whole body insulin sensitivity and insulin receptor tyrosine-kinase activity. *Diabetologia.* 40, 282-289.
18. **Ferron, M., Wei, J., Yoshizawa, T., DelFattore, A., DePinho, R. A., Teti, A., Ducy, P. and Karsenty, G.** (2010). Insulin signaling in osteoblasts integrates bone remodeling and energy metabolism. *Cell.* 142, 296-308.
19. **Fulzele, K., Riddle, R. C., DiGirolamo, D. J., Cao, X., Wan, C., Chen, D., Faugere, M. C., Aja, S., Hussain, M. A., Brüning, J. C., et al.** (2010). Insulin receptor signaling in osteoblasts regulates postnatal bone acquisition and body composition. *Cell.* 142, 309-319.
20. **González-Sánchez, J. L., Zabena, C., Martínez-Larrad, M. T., Martínez-Calatrava, M. J., Pérez-Barba, M. and Serrano-Ríos, M.** (2008). Association of ENPP1 (PC-1) K121Q polymorphism with obesity-related parameters in subjects with metabolic syndrome. *Clin Endocrinol (Oxf).* 68, 724-729.
21. **Goldfine, I. D., Maddux, B. A., Youngren, J. F., Reaven, G., Accili, D., Trischitta, V., Vigneri, R. and Frittitta L.** (2008). The role of membrane glycoprotein plasma cell antigen 1/ectonucleotide pyrophosphatase phosphodiesterase 1 in the pathogenesis of insulin resistance and related abnormalities. *Endocr Rev.* 29, 62-75.
22. **Huesa, C., Helfrich, M. H. and Aspden, R. M.** (2010). Parallel-plate fluid flow systems for bone cell stimulation. *J Biomech.* 43, 1182-1189.
23. **Harmey, D., Hessle, L., Narisawa, S., Johnson, K. A., Terkeltaub, R. and Millán, J. L.** (2004). Concerted regulation of inorganic pyrophosphate and osteopontin by akp2, enpp1, and ank: an integrated model of the pathogenesis of mineralization disorders. *Am J Pathol.* 164, 1199-1209.

24. **Hessle, L., Johnson, K. A., Anderson, H. C., Narisawa, S., Sali, A., Goding, J. W., Terkeltaub, R. and Millán, J. L**. (2002). Tissue-nonspecific alkaline phosphatase and plasma cell membrane glycoprotein-1 are central antagonistic regulators of bone mineralization. *Proc Natl Acad Sci USA.* 99, 9445-9449.
25. **Huesa, C., Yadav, M. C., Finnilä, M. A., Goodyear, S. R., Robins, S. P., Tanner, K. E., Aspden, R. M., Millán, J. L. and Farquharson, C.** (2011). PHOSPHO1 is essential for mechanically competent mineralization and the avoidance of spontaneous fractures. *Bone.* 48, 1066-1074.
26. **Johnson, K., Pritzker, K., Goding, J. and Terkeltaub, R.** (2001). The nucleoside triphosphate pyrophosphohydrolase isozyme PC-1 directly promotes cartilage calcification through chondrocyte apoptosis and increased calcium precipitation by mineralizing vesicles. *J Rheumatol.* 28, 2681-2691.
27. **Johnson, K., Goding, J., Van Etten, D., Sali, A., Hu, S. I., Farley, D., Krug, H., Hessle, L., Millán, J. L. and Terkeltaub, R.** (2003). Linked deficiencies in extracellular PP(i) and osteopontin mediate pathologic calcification associated with defective PC-1 and ANK expression. *J Bone Miner Res.* 18, 994-1004.
28. **Lacombe, J., Karsenty, G. and Ferron, M.** (2013). In vivo analysis of the contribution of bone resorption to the control of glucose metabolism in mice. *Molecular Metabolism.* 2, 498-504.
29. **Leslie, W. D., Rubin, M. R., Schwartz, A. V. and Kanis, J. A.** (2012). Type 2 diabetes and bone. *J Bone Miner Res.* 27, 2231-2237.
30. **Lee, N. K., Sowa, H., Hinoi, E., Ferron, M., Ahn, J. D., Confavreux, C., Dacquin, R., Mee, P. J., McKee, M. D., Jung, D. Y., et al.** (2007). Endocrine regulation of energy metabolism by the skeleton. *Cell.* 130, 456-469.
31. **Maddux, B. A and Goldfine, I. D.** (2000). Membrane glycoprotein PC-1 inhibition of insulin receptor function occurs via direct interaction with the receptor alpha-subunit. *Diabetes.* 49, 13-19.
32. **Mackenzie, N. C. W., Huesa, C., Rutsch, F. and MacRae VE.** (2012). New insights into NPP1 function: lessons from clinical and animal studies. *Bone.* 51, 961-968.
33. **Maddux, B. A., Chang, Y. N., Accili, D., McGuinness, O. P., Youngren, J. F. and Goldfine, I. D.** (2006). Overexpression of the insulin receptor inhibitor PC-1/ENPP1 induces insulin resistance and hyperglycemia. *Am J Physiol Endocrinol Metab.* 290, E746-749.
34. **Mackenzie, N. C. W., Zhu, D., Longley, L., Patterson, C. S., Kommareddy, S and MacRae, V. E.** (2011). MOVAS-1 cell line: a new in vitro model of vascular calcification. *Int J Mol Med.* 27, 663-668.
35. **McAteer, J. B., Prudente, S., Bacci, S., Lyon, H. N., Hirschhorn, J. N., Trischitta, V. and Florez, J. C.** (2008). The ENPP1 K121Q polymorphism is associated with type 2 diabetes in European populations: evidence from an updated meta-analysis in 42,042 subjects. *Diabetes.* 57, 1125-1130.
36. **Macrae, V. E., Horvat, S., Pells, S. C., Dale, H., Collinson, R. S., Pitsillides, A. A., Ahmed, S. F., and Farquharson, C.** (2009). Increased bone mass, altered

trabecular architecture and modified growth plate organization in the growing skeleton of SOCS2 deficient mice. *J Cell Physiol.* 218, 276-284.

37. **Mackenzie, N. C. W., Zhu, D., Milne, E. M., van 't Hof, R., Martin, A., Quarles, D. L., Millán, L. J., Farquharson, C. and MacRae, V. E.** (2012). Altered bone development and an increase in FGF-23 expression in Enpp1(-/-) mice. *PLoS One.* 7, e32177.
38. **Orriss, I. R, Burnstock, G. and Arnett, T.R.** (2010). Purinergic signalling and bone remodelling. *Curr. Opin. Pharmacol.* 10, 322–330.
39. **Parvathy, S. S. and Masocha, W.** (2013). Gait analysis of C57BL/6 mice with complete Freund's adjuvant-induced arthritis using the CatWalk system. *BMC Musculoskelet Disord.* 14, 14.
40. **Prudente, S., Morini, E. and Trischitta, V.** (2009). Insulin signaling regulating genes: effect on T2DM and cardiovascular risk. *Nat Rev Endocrinol.* 5, 682-693.
41. **Prosdocimo, D. A., Douglas, D. C., Romani, A. M., O'Neill, W. C. and Dubyak, G.R.** (2009). Autocrine ATP release coupled to extracellular pyrophosphate accumulation in vascular smooth muscle cells. *Am J Physiol Cell Physiol.*296, C828–C839.
42. **Pan, W., Ciociola, E., Saraf, M., Tumurbaatar, B., Tuvdendorj, D., Prasad, S., Chandalia, M. and Abate, N.** (2011). Metabolic consequences of ENPP1 overexpression in adipose tissue. *Am J Physiol Endocrinol Metab.* 301, E901-911.
43. **Pizzuti, A., Frittitta, L., Argiolas, A., Baratta, R., Goldfine, I. D., Bozzali, M., Ercolino, T., Scarlato, G., Iacoviello, L., Vigneri, R., Tassi, V., et al.** (1999). A polymorphism (K121Q) of the human glycoprotein PC-1 gene coding region is strongly associated with insulin resistance. *Diabetes.* 48, 1881-1884.
44. **Rosen C.J. and Motyl K.J**. (2010). No bones about it: insulin modulates skeletal remodeling. *Cell,* 142, 198-200.
45. **Ribeiro V., Garcia M., Oliveira R., Gomes P.S., Colaco B. and Fernandes M.H.** (2014). Bisphosphonates induce the osteogenic gene expression in co-cultured human endothelial and mesenchymal stem cells. *J Cell Mol Med,* 18, 27-37.
46. **Stentz, F. B. and Kitabchi, A. E.** (2007). Transcriptome and proteome expressions involved in insulin resistance in muscle and activated T-lymphocytes of patients with type 2 diabetes. *Genomics Proteomics Bioinformatics.* 5, 216-235.
47. **Stefan, C., Jansen, S. and Bollen, M.** (2000). NPP-type ectophosphodiesterases: unity in diversity. *Trends Biochem Sci.* 30, 542-550.
48. **Staines, K. A., Zhu, D., Farquharson, C. and MacRae, V. E.** (2013). Identification of novel regulators of osteoblast matrix mineralization by time series transcriptional profiling. *J Bone Miner Metab.* 32, 240-251.
49. **Sali, A., Favaloro, J. M., Terkeltaub, R. and Goding, J. W.** (1999). Germline deletion of the nucleoside triphosphate pyrophosphohydrolase (NTPPPH) plasma cell membrane glycoprotein-1 (PC-1) produces abnormal calcification of periarticular tissues. *Ecto-ATPases and Related Ectoenzymes* (ed. L. Vanduffel and R. Lemmens), pp. 267–282. The Netherlands: Shaker Publishing.

50. **Stolerman, E. S., Manning, A. K., McAteer, J. B., Dupuis, J., Fox, C. S., Cupples, L. A., Meigs, J. B. and Florez, J. C.** (2008). Haplotype structure of the ENPP1 Gene and Nominal Association of the K121Q missense single nucleotide polymorphism with glycemic traits in the Framingham Heart Study. *Diabetes.* 57, 1971-1977.
51. **Terkeltaub, R. A. (2001).** Inorganic pyrophosphate generation and disposition in pathophysiology. *Am J Physiol Cell Physiol*. 281, C1-C11.
52. **Terkeltaub, R.** (2006). Physiologic and pathologic functions of the NPP nucleotide pyrophosphatase/phosphodiesterase family focusing on NPP1 in calcification. *Purinergic Signal.* 2, 371-377.
53. **Teno, S., Kanno, H., Oga, S., Kumakura, S., Kanamuro, R. and Iwamoto, Y.** (1999). Increased activity of membrane glycoprotein PC-1 in the fibroblasts from non-insulin-dependent diabetes mellitus patients with insulin resistance. *Diabetes Res Clin Pract.* 45, 25-30.
54. **Vaingankar, S. M., Fitzpatrick, T. A., Johnson, K., Goding, J. W., Maurice, M. and Terkeltaub, R.** (2004). Subcellular targeting and function of osteoblast nucleotide pyrophosphatase phosphodiesterase 1. *Am J Physiol Cell Physiol.* 286, C1177-1187.
55. **Zimmermann, H., Zebisch, M. and Sträter N.** (2012). Cellular function and molecular structure of ecto-nucleotidases. *Purinergic Signal.* 8,437-502.
56. **Zhuo, Q., Yang, W., Chen, J. and Wang, Y.** (2012). Metabolic syndrome meets osteoarthritis. *Nat. Rev. Rheumatol.* 8, 729-737.
57. **Zhu, D., Mackenzie, N. C. W., Millán, J. L., Farquharson, C. and MacRae, V. E.** (2011). The appearance and modulation of osteocyte marker expression during calcification of vascular smooth muscle cells. *PLoS One.* 6, e19595.
58. **Zhu, D., Mackenzie, N. C. W., Millan, J. L., Farquharson, C. and MacRae, V. E.** (2013). A protective role for FGF-23 in local defence against disrupted arterial wall integrity? *Mol Cell Endocrinol.* 372, 1-11.
59. **Zhou, H. H., Chin, C. N., Wu, M., Ni, W., Quan, S., Liu, F., Dallas-Yang, Q., Ellsworth, K., Ho, T., Zhang, A., et al.** (2009). Suppression of PC-1/ENPP-1 expression improves insulin sensitivity in vitro and in vivo. *Eur J Pharmacol.* 616, 346-352.

Figure legends

Figure 1. *Enpp1*$^{-/-}$ mice significant muscle reduction but not significant changes in fat mass. A) Body weight (g) growth curves for *Enpp1*$^{-/-}$ and WT mice (n=6). *Enpp1*$^{-/-}$ mice show reduced B) Quadratus femoris and C) Soleus muscle weight relative to total body weight (mg/g), compared with WT controls (n=6). D) Walking gait stride length of *Enpp1*$^{-/-}$ and WT mice (n=4). E) Subcutaneous, messenteric, gonadal and brown fat pad weight relative to total body weight (mg/g) compared to WT controls (n=6). Relative expression of WAT markers and *Insr* in F) subcutaneous and G) gonadal fat pad. Mice were reared under control dietary conditions and were 18 weeks of age at the time of dissection. Results are presented as mean ± SEM * P<0.05, ** P<0.01, *** P<0.001.

Figure 2. *Enpp1*$^{-/-}$ mice exhibit insulin sensitization. A) Glucose tolerance test (GTT). B) Glucose stimulated insulin secretion (GSIS). C) Insulin tolerance test (ITT) represented as percentage (%) of basal glucose. D) Metabolic tests analyzed as area under the curve. Mice were reared under control dietary conditions to 16 weeks of age. Results are presented as mean ± SEM (n=8) *P<0.05.

Figure 3. *Enpp1*$^{-/-}$ mice show pronounced obesity-resistance in response to a chronic high fat diet challenge. *Enpp1*$^{-/-}$ and WT mice were reared on a high fat diet from 4 weeks of age. A) Body weight (g) growth curves (n=16). B) Body weight (g) at 18 weeks of age (n=8). C) Walking gait stride length in WT and *Enpp1*$^{-/-}$ mice (n=4). D) WAT weight analysis in ratio to total body weight (mg/g) (n=8). E) Maximum gonadal fat cell diameter (n=4). F) BAT weight analysis in ratio to total body weight (n=8). Gene expression of WAT and BAT markers and *Insr* in G) subcutaneous and H) gonadal fat pad. I) Histological oil red O staining of lipid deposits in cryosections of the liver. Mice were analyzed at 18 weeks of age after 14 weeks under high fat dietary conditions. Results are presented as mean ± SEM *P<0.05, ** P<0.01, *** P<0.001, NS: non-significant.

Figure 4. *Enpp1*$^{-/-}$ mice show improved insulin tolerance in response to a chronic high fat diet challenge. A) Glucose tolerance test (GTT), B) Glucose stimulated insulin secretion (GSIS) and C) Insulin tolerance test (ITT) represented as percentage (%) of basal glucose. Mice were reared under high fat dietary conditions and were 16 weeks of age. Results are

presented as mean ± SEM (n=7) *P<0.05. D) Metabolic tests analyzed as area under the curve. E) Number of islets. F) Size of islets. Results are presented as mean ± SEM *P<0.05.

Figure 5. Metabolic effects in *Enpp1*$^{-/-}$ mice are independent of bone insulin signaling but associated with altered osteocalcin carboxylation status. A) Immunofluorescent staining of the insulin receptor on the surface of wild type and *Enpp1*$^{-/-}$ neonatal calvarial primary osteoblast cultures. B) Relative mRNA expression levels of *Insr* in calvarial osteoblast cultures (n=6). C) Representative immunoblots demonstrating the effects of insulin (INS; 10 nM) and IGF-1 (10 nM) on the phosphorylation of Akt, Glycogen synthase kinase-3 beta (GSK-3β) and Erk1/2 in calvarial osteoblasts cultures (n≥3). Measurement of serum D) total osteocalcin, E) carboxylated osteocalcin, F) undercarboxylated osteocalcin, G) uncarboxylated osteocalcin, H) bone formation marker P1NP and I) bone resorption marker CTX-I in 6 and 12 week old mice. Results are presented as mean ± SEM (n=6) *P<0.05.

Figure 6. High fat diet induces a deterioration of trabecular bone architecture. Representative images of trabecular bone from 18 week old mice tibiae. A) WT control diet. B) *Enpp1*$^{-/-}$ control diet. C) WT high fat diet. D) *Enpp1*$^{-/-}$ high fat diet. E) Bone formation marker P1NP and F) bone resorption marker CTX-I in 6 and 12 week old mice. Results are presented as mean ± SEM (n=6) *P<0.05, *** P<0.001.

Figure 7. Schematic representation of the effects of NPP1 on bone mineralization, obesity and glucose intolerance. NPP1 hydrolyses ATP to generate pyrophosphate (PPi), which is a key inhibitor of mineralization. Global deletion of *Enpp1* results in decreased PPi levels, leading to ectopic calcification of blood vessels and cartilage. However, in lone bones, *Enpp1* ablation leads to insufficient PPi substrate for TNAP to generate Pi for normal mineral formation. On the other hand, decreased PPi may reduce the ratio of OPG to RANKL, resulting in increased bone resorption by osteoclasts (Ribeiro et al., 2014). The acidic pH (4.5) in resorption lacunae decarboxylates osteocalcin (GLA-OCN) stored in the bone extracellular matrix to generate undercarboxylated active osteocalcin (GLU13-OCN), which stimulates insulin secretion by the β-cells of the pancreatic islets and promotes insulin sensitivity (Ferron and Lacombe, 2014). Increased insulin binds to the insulin receptor in osteoblasts and inhibits the expression of OPG, driving osteoclastic bone resorption and the further release of GLU13-OCN. Increased insulin secretion protects high fat diet induced obesity and glucose intolerance, and impacts on insulin sensitive tissues, such as muscle and

adipose. Additionally, GLU13-OCN may directly stimulate energy consumption in skeletal muscle and adipose tissue and may decrease lipid accumulation in the liver (Rosen and Motyl, 2010).

Translational Impact:

Clinical issue:

More than half a billion individuals worldwide suffer from obesity and its associated metabolic disease, such as type 2 diabetes. The emergence of bone as an endocrine regulator leads to revaluate the role of bone mineralization factors in the development of metabolic disease. Despite the recognized importance of Ectonucleotide pyrophosphatase/phosphodiesterase-1 (NPP1) in the regulation of bone mineralization, its contribution to obesity and type 2 diabetes remains less clear.

Results:

This research investigated the association of the metabolic phenotype and impaired bone metabolism in mice lacking the NPP1 gene (*Enpp1*$^{-/-}$ mice). The authors provide new evidence that *Enpp1*$^{-/-}$ mice showed a pronounced resistance to obesity and insulin resistance in response to chronic high fat feeding. Furthermore, the authors show that *Enpp1*$^{-/-}$ mice had increased levels of the insulin sensitising bone-derived hormone osteocalcin, although insulin signaling remains unchanged within osteoblasts.

Implications and future directions:

These findings shed more light on the important role of NPP1 in the development of obesity and type 2 diabetes and provide information on the mechanism by which this protein regulates insulin sensitivity. A fuller understanding of the pathways of NPP1 may inform the development of novel therapeutic strategies for treating insulin resistance.

	Parameter	Control diet		High fat diet	
		WT (n=6)	*Enpp1*$^{-/-}$ (n=6)	WT (n=8)	*Enpp1*$^{-/-}$ (n=6)
Trabecular bone	Percentage bone volume	13.05 ± 4.388^{b}	7.70 ± 2.101^{b}	9.10 ± 3.119	5.36 ± 2.556
	Trabecular thickness (µm)	50.8 ± 7.5	56.5 ± 6.1^{b}	47.6 ± 3.30	47.6 ± 4.7
	Trabecular separation (µm)	214.1 ± 56.2	280.1 ± 50.1	247.5 ± 60.31	289.4 ± 80.9
	Trabecular number (µm^{-1})	0.00266 ± 0.00102	0.00137 ±0.00039^{a}	0.00196 ± 0.0007778	0.00115 ± 0.00060^{a}
	Trabecular pattern factor	0.0255 ± 0.0075	0.0338 ± 0.00597^{a,b}	0.0319 ± 0.004003	0.0419 ± 0.0066^{a,b}
	Structure model index	2.19 ± 0.56	2.74 ± 0.27^{a,b}	2.38 ± 0.279	2.77 ± 0.34
	Degree of anisotropy	2.44 ± 0.29^{b}	2.51 ± 0.15^{b}	2.20 ± 0.201	2.24 ± 0.40
Cortical bone	Bone Mineral Density (g/cm^{3})	1.29 ± 0.02^{b}	1.31 ± 0.04	1.34 ± 0.02	1.32 ± 0.02
	Cortical thickness (µm)	176.03 ± 15.49	175.61 ± 6.33^{b}	181.35 ± 6.64	157.01 ± 13.00^{a,b}
	Cortical porosity (%)	2.14 ± 0.61	1.94 ± 0.44	2.08 ± 0.51	1.99 ± 0.29
	Maximum Stiffness (N/mm)	54.77 ± 6.06	49.09 ± 3.30^{a}	49.09 ± 3.83	48.66 ± 4.13
	Work to failure (N·mm)	3.09 ± 1.12	2.26 ± 0.41	2.26 ± 0.44	2.33 ± 0.75
	Work to fracture (N·mm)	9.21 ± 2.44^{b}	7.60 ± 1.58^{a,b}	7.60 ± 1.46	4.99 ± 0.10^{a,b,c}
	Work post-failure (N·mm)	5.92 ± 1.80^{b}	5.29 ± 1.43^{a,b}	5.29 ± 1.38	2.62 ± 0.72^{a,b,c}

Table 1: Chronic high fat diet challenge induces an enhanced deterioration of trabecular bone architecture and exacerbates the disrupted bone mineralization phenotype of *Enpp1*$^{-/-}$ mice. Trabecular bone parameters were measured by µCt on 18 week old male tibiae. Results are presented as mean ± SD. Significant differences (P<0.05) a same diet vs WT, b same genotype vs high fat diet. Cortical bone parameters were measured by µCt on 18 week old male tibiae. The same bones were then tested for biomechanical properties by 3 point bending. Results are presented as mean ± SD. Significant differences (P<0.05) a same diet vs WT, b same genotype vs high fat diet, c vs different genotype and different diet.

Fig.1

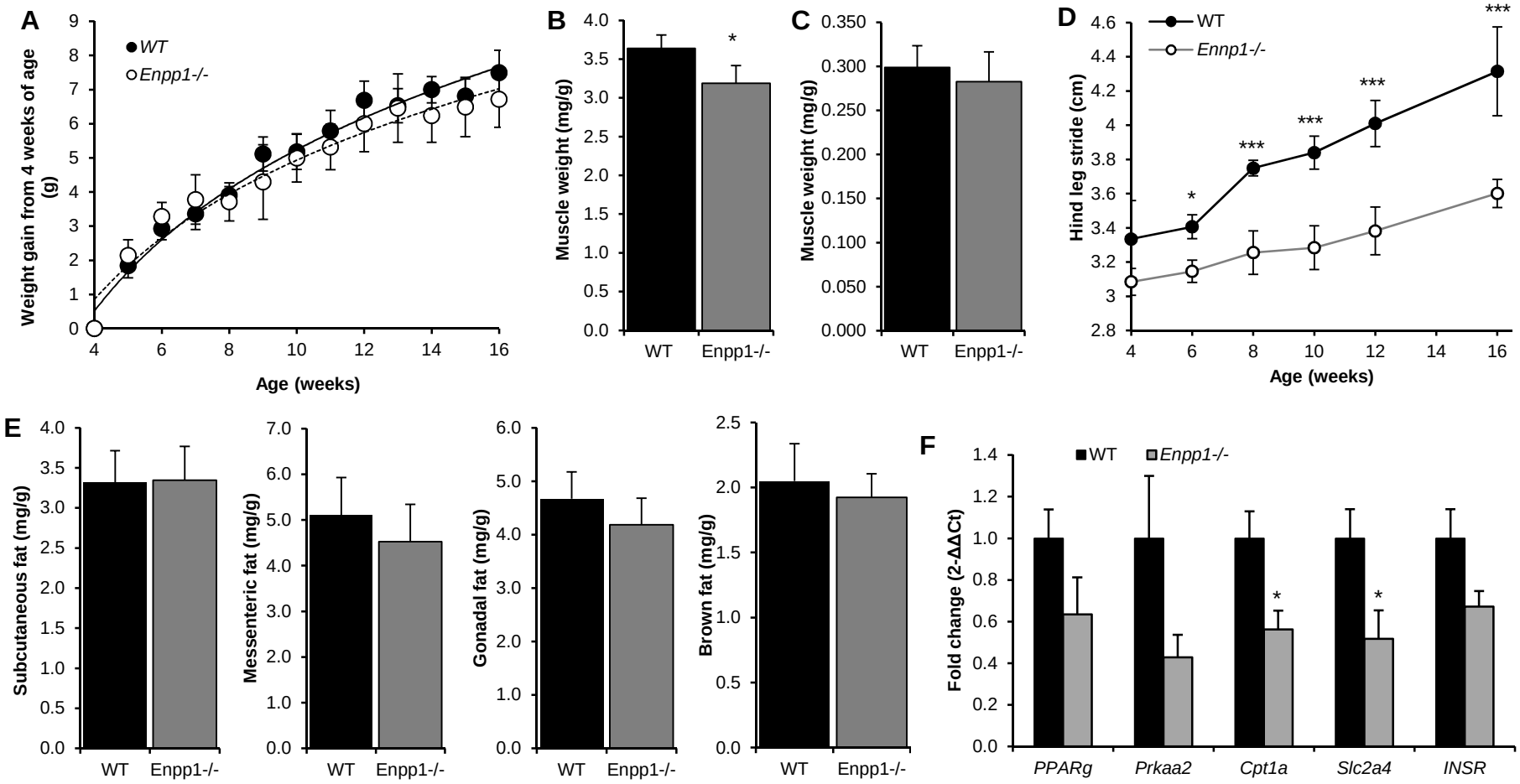
A
WT
Enpp1-/-
Weight gain from 4 weeks of age (g)
Age (weeks)
B
Muscle weight (mg/g)
WT
Enpp1-/-
C
Muscle weight (mg/g)
WT
Enpp1-/-
D
WT
Ennp1-/-
Hind leg stride (cm)
Age (weeks)
E
Subcutaneous fat (mg/g)
Messenteric fat (mg/g)
Gonadal fat (mg/g)
Brown fat (mg/g)
WT
Enpp1-/-
F
WT
Enpp1-/-
Fold change (2-ΔΔCt)
PPARg
Prkaa2
Cpt1a
Slc2a4
INSR

Fig.2

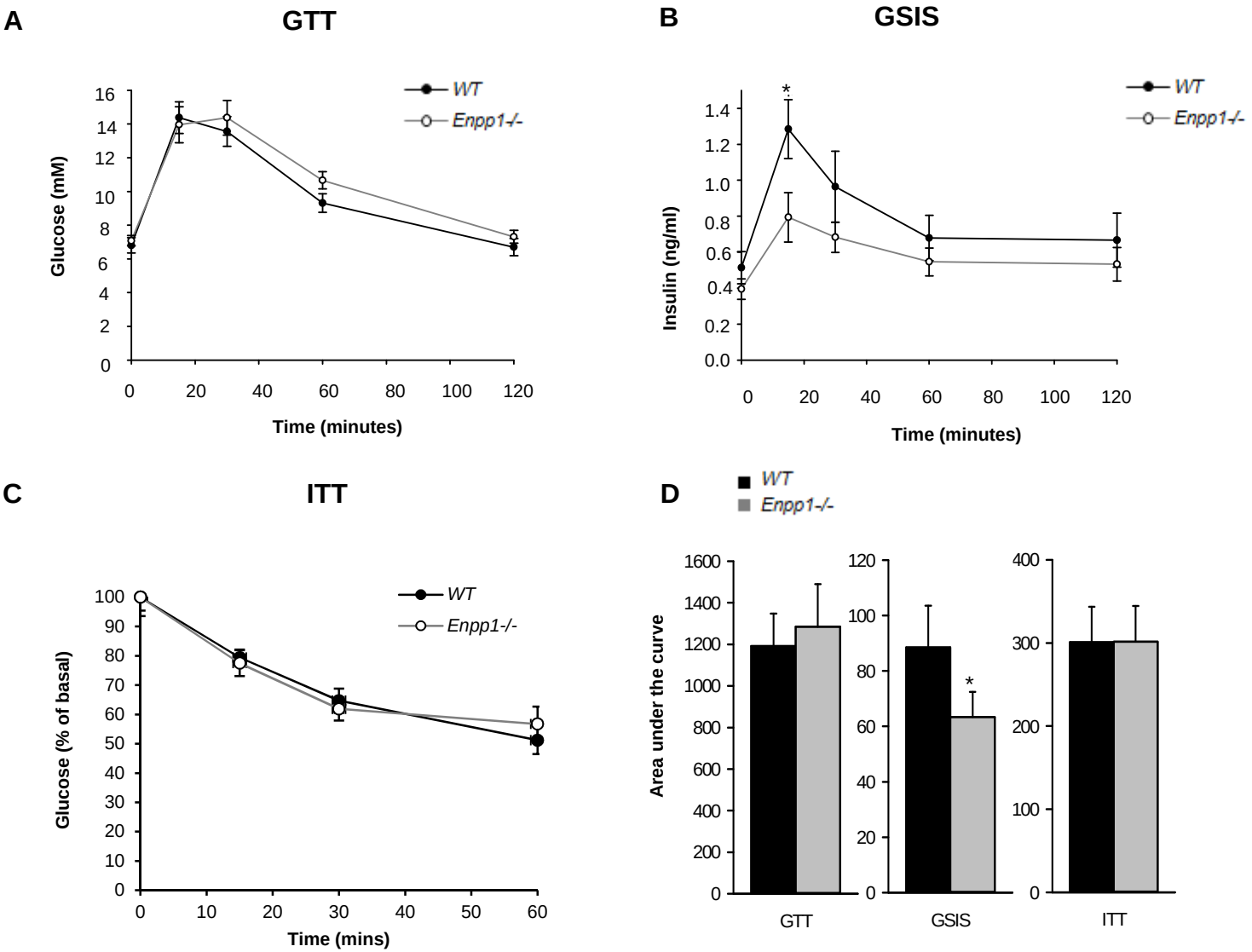
A
GTT
WT
Enpp1-/-
Glucose (mM)
Time (minutes)
B
GSIS
*
Insulin (ng/ml)
Time (minutes)
C
ITT
Glucose (% of basal)
Time (mins)
D
Area under the curve
GTT
GSIS
ITT

Fig.3

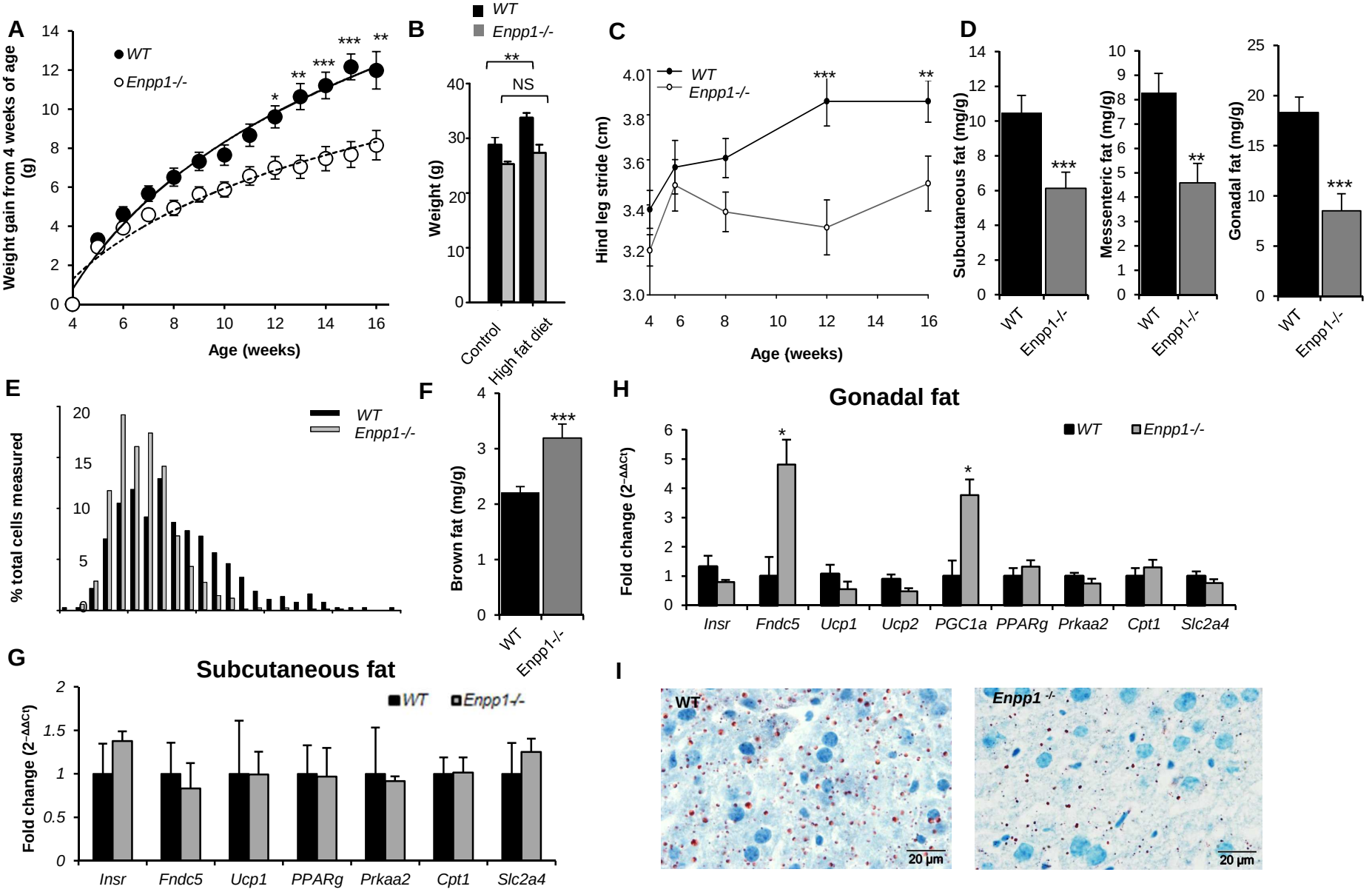
A
Weight gain from 4 weeks of age (g)
WT
Enpp1-/-
Age (weeks)
B
WT
Enpp1-/-
Weight (g)
NS
Control
High fat diet
C
Hind leg stride (cm)
WT
Enpp1-/-
Age (weeks)
D
Subcutaneous fat (mg/g)
Messenteric fat (mg/g)
Gonadal fat (mg/g)
WT
Enpp1-/-
E
% total cells measured
WT
Enpp1-/-
F
Brown fat (mg/g)
WT
Enpp1-/-
G
Subcutaneous fat
Fold change (2-ΔΔCt)
WT
Enpp1-/-
Insr
Fndc5
Ucp1
PPARg
Prkaa2
Cpt1
Slc2a4
H
Gonadal fat
Fold change (2-ΔΔCt)
WT
Enpp1-/-
Insr
Fndc5
Ucp1
Ucp2
PGC1a
PPARg
Prkaa2
Cpt1
Slc2a4
I
WT
Enpp1 -/-
20 µm
20 µm

Fig.4

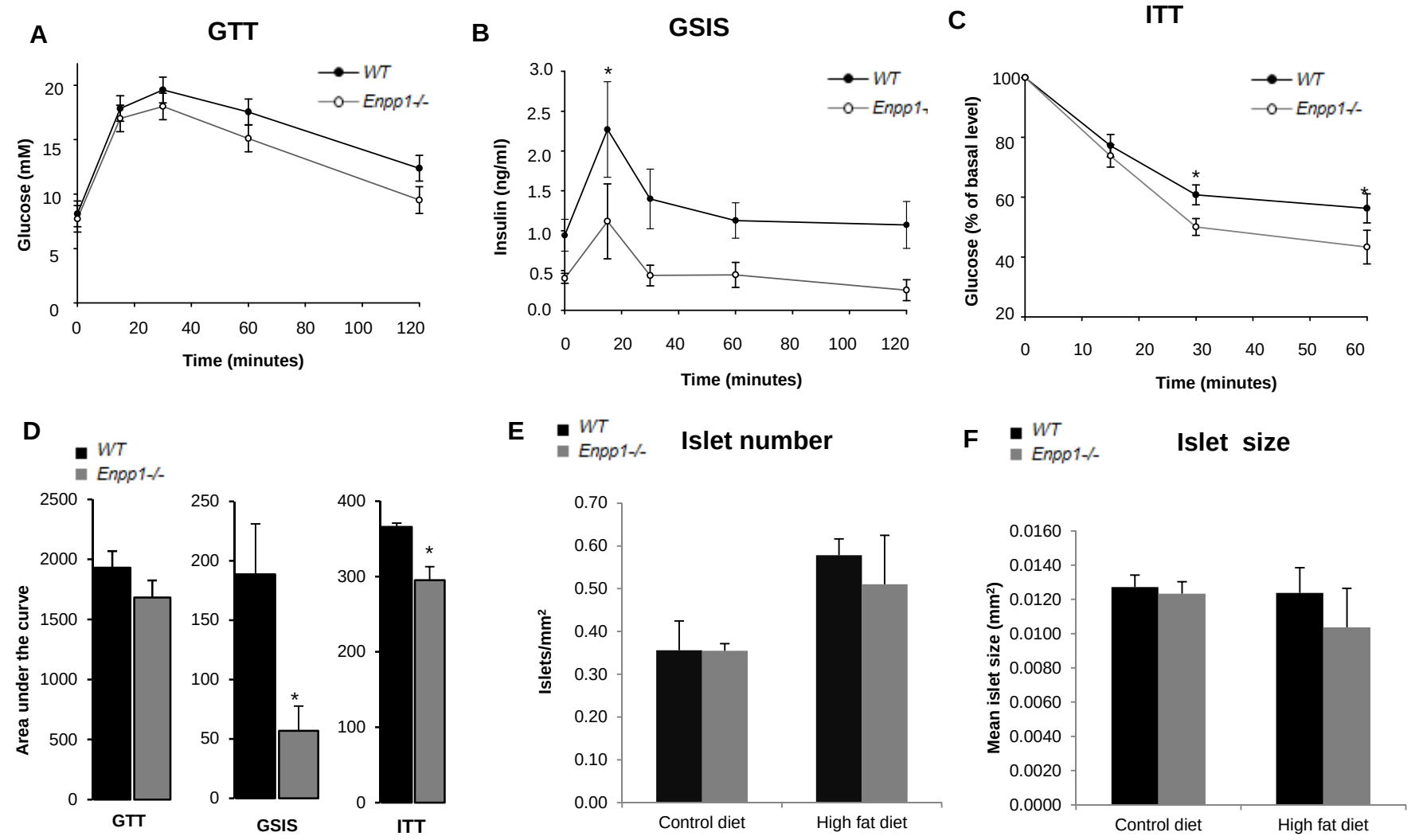
A
GTT
WT
Enpp1-/-
Glucose (mM)
Time (minutes)
B
GSIS
Insulin (ng/ml)
Time (minutes)
C
ITT
Glucose (% of basal level)
Time (minutes)
D
Area under the curve
GTT
GSIS
ITT
E
Islet number
Islets/mm²
Control diet
High fat diet
F
Islet size
Mean islet size (mm²)
Control diet
High fat diet

Fig.5

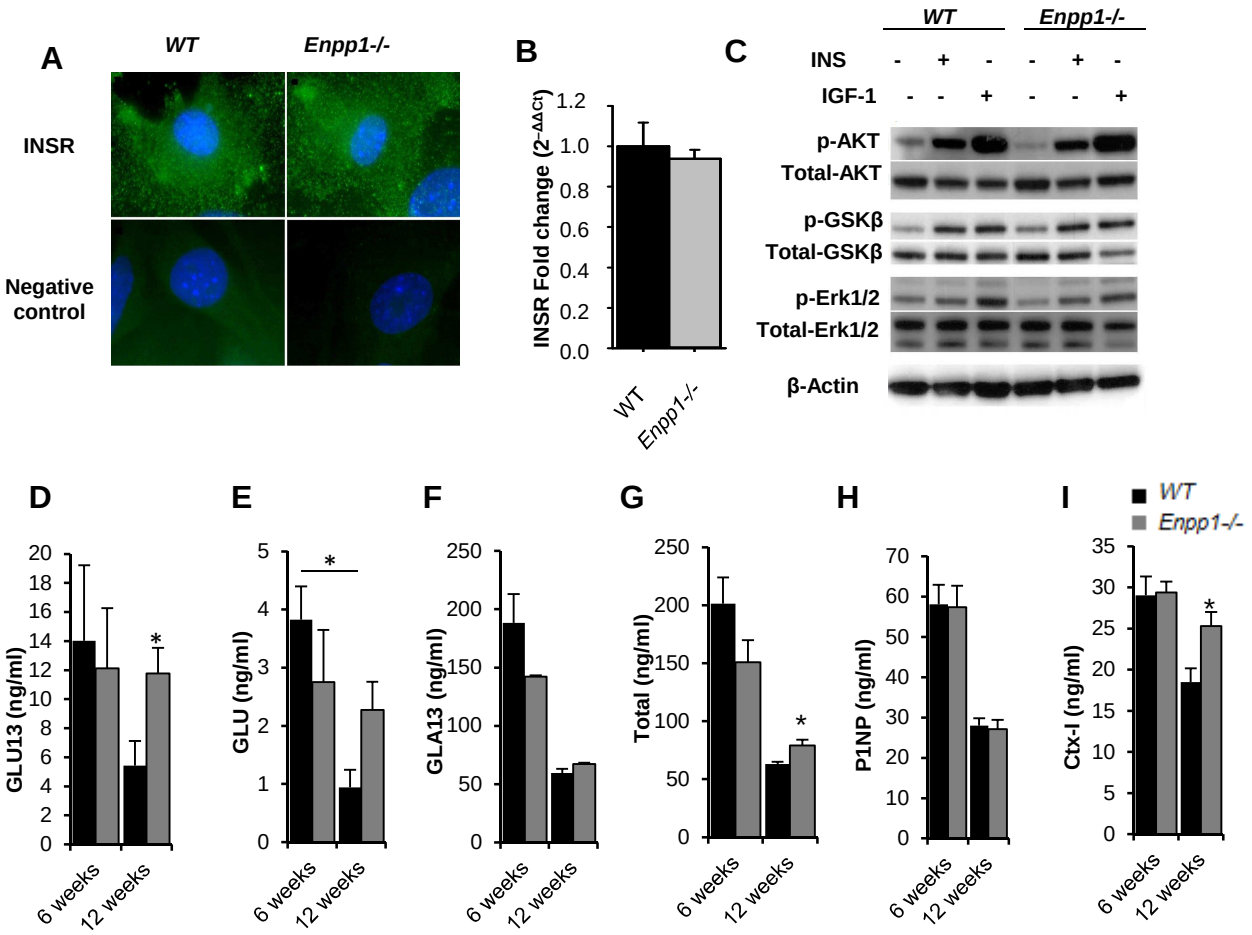
A
WT
Enpp1-/-
INSR
Negative control
B
INSR Fold change (2-ΔΔCt)
1.2
1.0
0.8
0.6
0.4
0.2
0.0
WT
Enpp1-/-
C
WT
Enpp1-/-
INS - + - - + -
IGF-1 - - + - - +
p-AKT
Total-AKT
p-GSKβ
Total-GSKβ
p-Erk1/2
Total-Erk1/2
β-Actin
D
GLU13 (ng/ml)
E
GLU (ng/ml)
F
GLA13 (ng/ml)
G
Total (ng/ml)
H
P1NP (ng/ml)
I
WT
Enpp1-/-
Ctx-I (ng/ml)
6 weeks
12 weeks
*

Fig.6

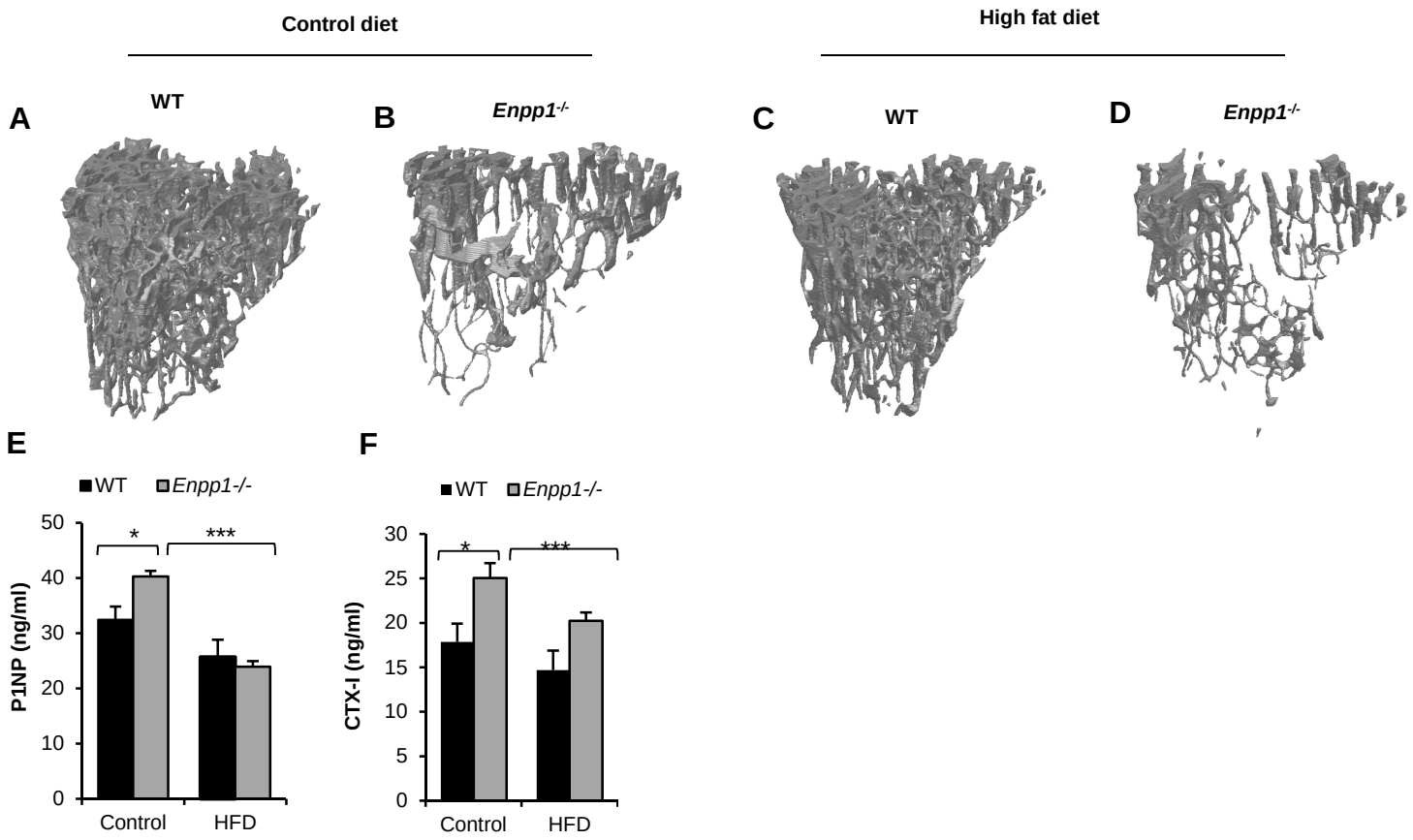
Control diet
High fat diet
A
WT
B
Enpp1-/-
C
WT
D
Enpp1-/-
E
WT
Enpp1-/-
P1NP (ng/ml)
50
40
30
20
10
0
*
***
Control
HFD
F
WT
Enpp1-/-
CTX-I (ng/ml)
30
25
20
15
10
5
0
*
***
Control
HFD

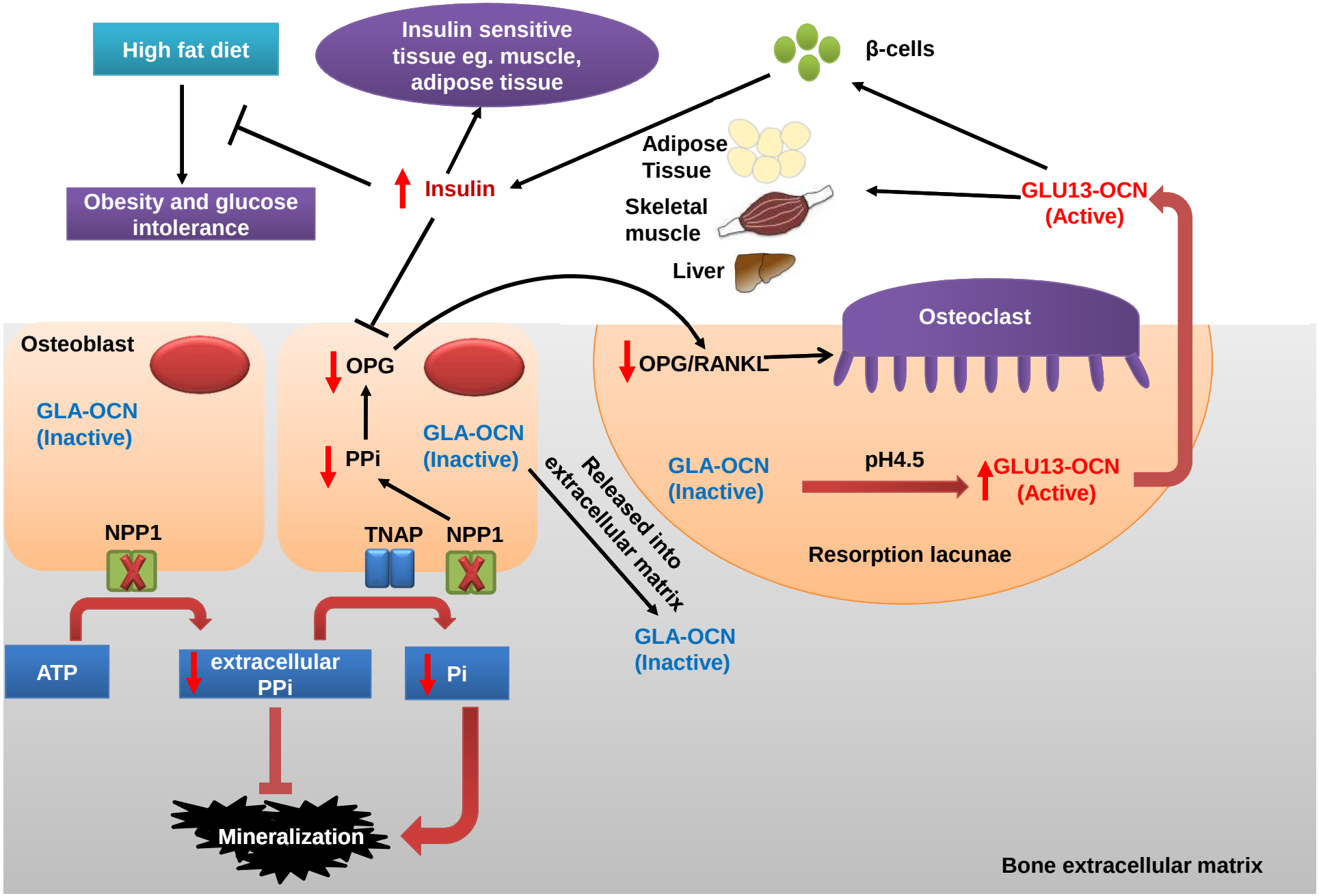
High fat diet
Insulin sensitive tissue eg. muscle, adipose tissue
β-cells
Obesity and glucose intolerance
Insulin
Adipose Tissue
Skeletal muscle
Liver
GLU13-OCN (Active)
Osteoblast
GLA-OCN (Inactive)
OPG
PPi
GLA-OCN (Inactive)
OPG/RANKL
Osteoclast
GLA-OCN (Inactive)
pH4.5
GLU13-OCN (Active)
Resorption lacunae
Released into extracellular matrix
NPP1
TNAP
NPP1
ATP
extracellular PPi
Pi
GLA-OCN (Inactive)
Mineralization
Bone extracellular matrix